Journal of Information Systems Engineering and Management
2025, 10(27s)
e-ISSN: 2468-4376

https://www.jisem-journal.com/

Research Article

Deep Learning-Based OSIS-NET Framework for Accurate Detection and Classification of Osteoporosis Using MRI Imaging and Advanced Machine Learning Techniques

Dr.Sheena A.D[1], D. Divya Sterlin[2], Sindhuja. K [3], Kuppan.P[4], Dr.Vishwa Priya. V[5], Dr.Sangeetha Radhakrishnan[6], Dr. D. Padma Priya[7*], Dr.M.Yogeshwari[8]

[1]*Department of Civil Engineering, Vels Institute of Science and Technology and Advanced Studies (VISTAS), Chennai, mail id: dr.sheenaad@gmail.com.*

[2]*Department of E-edu Govern Department, S.D.N.B.Vaishnav College For Women, Chennai, mail.id : ddsterlin@gmail.com*

[3]*Department of Computer Science, SRM University , Ramapuram , Chennai, Mail.id: sindhujk@srmist.edu.in* [4]*Department of Computer science, VISTAS,Chennai. Mail.id: kuppan.anj@gmail.com*

[5]*Department of Computer Science, Vels Institute of Science and Technology and Advanced Studies (VISTAS), Chennai, mail id: vishwapriya13@gmail.com*

[6] *Department of Computer Science, Vels Institute of Science and Technology and Advanced Studies (VISTAS), Chennai, mail id: Sangeetha0988@gmail.com*

[7*] *Department of Techcom and Performing Arts, Saveetha liberal Arts and Science College, Saveetha University, Corresponding Author: Padmapriyad.sclas@saveetha.com*

[8] *Department of Data Analyst, Saveetha liberal arts and Science College , Saveetha University, mail.id: yogisarainteract@gmail.com*

ARTICLE INFO

Received: 18 Dec 2024

Revised: 15 Feb 2025

Accepted: 28 Feb 2025

ABSTRACT

Osteoporosis manifests in people as a painful bone disease which causes weakness because of reduced bone density and breakdown. A predictive diagnosis of osteoporosis and fragility fractures becomes possible during the first years of menopause. Two different types of bone loss in women develop osteoporosis through both menopause-related sources and external factors. DEXA diagnostic tools fail to demonstrate the intricate bone structural changes that occur in tissues effectively. This document proposes the implementation of OSIS-NET which detects and classifies osteoporosis conditions using deep learning principles. A collection of MRI images originates from the OASIS-3 Datasets followed by noise reduction using adaptive gaussian trilateral filter for artifact removal. The Sobel edge detector receives the images which underwent denoising to produce specific and detailed edges in dual images. The next stage applies deep learning (DL) based Dilated leaky ShuffleNet to process images for extracting textural and shape features from them. The selected ST features undergo an evaluation process using ML models which includes SVM, KNN, DT, and RF for detecting normal and abnormal patterns. The system reaches an excellent accuracy level that exceeds 99.76% for normal cases and 99.89% for abnormal cases. The model achieves 0.86% superior accuracy when compared to GoogleNet alongside 0.54% and 0.16% and 1.07% superior results than ShuffleNet, AlexNet and MobileNet respectively.

Keywords: Osteoporosis detection, Dilated leaky ShuffleNet, Adaptive Gaussian Trilateral Filter, SVM.

INTRODUCTION

Osteoporosis remains a medical condition that disorders bone tissues making them lose mass, and declining their architecture [1]. This is an important reason as well as frequent ailments of the skeletal system that might have a metabolic cause, and characterized by the increased risk of fractures [2]. One of the potential hazards that cause osteoporosis in women after some age is menopause. Post-menopausal women are acknowledged to lose about 2% , 5% of cortical , trabecular bone per year during the 1st five to eight years of their menopause [3]. Bone loss in women is of two sorts which causes osteoporosis: It can be said that it is menopause related or it depends on menopause [4]. Most severe cases also lead to diseases that increase the likelihood of dying. Osteoporosis affects millions of people every year, and this menace rises in the global population due to the aging population caused by the increase in life

span as observed recently [5]. The primary type of osteoporosis usually impacts the people over the age of 65. The survey of the nationwide and multicentre showed that the prevalence of osteoporosis in people over 50 years was 6.46% for man and 29.13% for woman in China [6]. Osteopenia is another factor in fragility fractures and the condition comes before osteoporosis. In various researches that focused on osteopenia findings have shown that the most affected girls were those that have fractured in fragility [7]. At the same time, most of osteopenia and osteoporosis are untapped until the patient has a fracture, therefore increases the risk of complications and mortality [8]. However, osteoporosis begins and often does no show symptoms in the early stage hence it can easily go unnoticed [9].

DXA is considered to be a reliable technique for establishing the prevalence of osteoporosis in particular and for determining BMD in general [10]. DXA scans are another type of inspecting form that are not suitable for general use due to their costly nature [11]. The US Preventive Task Force of Osteoporosis fracture prevention has endorsed BMD screening [12]. Several treatments aimed at using therapeutic drugs are more effective before the fractures set .Although DEXA scan can be routinely used for BMD assessment, they are two-dimensional scans which might not assess the structural or morphological changes in the third dimension or the quality of the bones, which is very important in figuring out the high risk fractures [14, 15]. This might result in lack of diagnosis in first stages of osteoporosis, or rating of similar patients who have the same bone mass density but different bone fragility. In addition, some of the sources of error include differences in the equipment used in taking images, how the patient is positioned and the experience of the person operating the equipment among others. Given this a new OSIS-NET for accurate detection and classification of osteoporosis has been developed by adopting deep learning methods. His/Her research contribution can be highlighted as follows:

- Initially, the MRI images are gathered from the publicly available SpineWeb Datasets and pre-processed using adaptive gaussian trilateral filter to denoise the noisy artifacts.
- The noise-free images are fed into the Sobel edge detector to generated the specific and fined edges in the dual images.
- Then the images are fed into deep learning (DL) based Dilated leaky ShuffleNet for extracting the textural features and generated edges for extracting the shape features.
- Finally, the selected ST features are evaluated using several machine learning (ML) models, including SVM, KNN, DT and RF for classifying the normal and abnormal cases.

This following are the research's sections organized as follows: Section II provides into further detail about the literature review. Section III provides the suggested course of action. The result is shown within Section IV, V provides details of the conclusion.

LITERATURE SURVEY

This section presents osteoporosis detection and classification based on DL and ML image analysis.

It was suggested in 2020 by Aliaga, I., et al [16] an automatic technique to identify specific marks and lines on panoramic radiographs of teeth. Therefore, it is attempted to find out relevant mandibular indices for thinning and decay of mandibular bone. The validity of the suggested technique was confirmed based on the statistical research with bone structure deterioration analysis with different levels of osteoporosis and qualitatively evaluated against the standard of skilled dentists. The advantage of this approach is that it is sufficiently resilient in that all indices are calculated for two flexible size and location regions of interest.

A U-NET based enhanced osteoporosis detection algorithm was developed by Liu, J., et al [17], 2020. After that, each segmented images is extracted and the diagnostic result is obtained. The experimental results show that the enhanced U-net is capable of accurately tackling the effect of picture interference during the bone mineral density measuring process. The U-net automatic diagnosis approach outperforms other comparable methods in terms of diagnosis effect and recognition rate, with a rate above 81%.

Recently, in 2021, Fang, Y., et al [18] proposed a fully automated method for BMD analysis and vertebral body segmentation from CT with DCNNs. Type of convolutional neural network used to evaluate the BMD was a DenseNet-
121. The values obtained from the quantitative computed tomography (QCT) post processing were determined to be

the standards for analysis. Deep learning techniques can be applied to achieve fully automatic diagnosis of normal bone mineral density, osteopenia and osteoporosis from CT images.

Tang, C., et al. [19] suggested in 2021 that CNN based approach mainly consists of two functional modules, which analyze the diagnostic 2D CT slice to accomplish the qualitative BMD detection. As a result, based on network findings, the radiologists provide preliminary qualitative results for BMD diagnosis. Finally, the suggested MS-Net is able to guarantee both computation and memory efficiencies thus allowing us to keep the morphology of various lumbar vertebrae. The suggested BMDC-Net was 76.65% accurate and it had the receiver operating characteristic area of 0.9167.

For an example, in 2022, Wang, Y., proposed [20] proposing that the multi modal semantic consistency network based on the semantic consistency properties of CT could work well in classifying X ray OVFs. In this regard, different from the previous approaches, the domain soft labels are provided by a feature level mix up module that reduces the domain offset for network between X-ray and CT. In order to help learning of the high level semantic invariant properties in the X-ray and CT domains, the neural network employs a self rotation training task as a pretext to its training. The best AUC value is raised from 86.32 to 92.16% according to the final results using this strategy.

Widyaningrum, R., et al [21] developed an automated trabecular bone segmentation technique in 2024 that used 60 training datasets and 120 areas of interests in periapical radiographs to split into 42 testing datasets. Machine learning and color histogram are applied for the diagnosis of osteoporosis. In order to diagnose osteoporosis, BMD is measured by using the dual X-ray absorptiometry techniques. It particularly improves the field of osteoporosis diagnosis based on medical image analysis and can be further refined for use in the field of dentistry.

D.H. Hwang, et al [22] presented a multi-view CT network (MVCTNet) in 2024 in which two images from the original CT images are used to automatically classify osteopenia and osteoporosis. It consists of a classification challenge on detecting osteoporosis or osteopenia from CT images. Both the quantitative and qualitative evaluations conclude that the recommended approach increases the performance of each trial.

PROPOSED METHOD:

This study develops a new OSIS-NET system to detect and sort osteoporosis cases using deep learning methods. The research team obtains MRI images from OASIS-3 Data Sets as public records before applying an adaptive gaussian trilateral filter for denoising unwanted image artifacts. The cleaned images enter the Sobel edge detector software to produce accurate edge definition across both images. The system sends MRI images to Dilated leaky ShuffleNet to generate textural and feature outlines from them. After gathering significant ST features the next step involves analyzing them with multiple ML methods including SVM, KNN, DT and RF to separate normal from abnormal cases. The figure 1 presents the design of our OSIS-NET system.

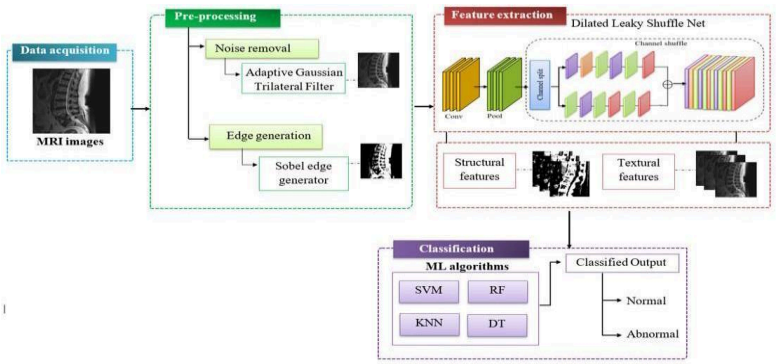

Figure 1: Proposed OSIS-NET method.

Adaptive Gaussian Trilateral Filter:

The Adaptive Gaussian trilateral filter is used during preprocessing to eliminate noise artifacts from the input medical images. It implements the bilateral filter's fundamental values into practice. The following pixels are averaged using weights determined by their distances from the original pixel in order to perform the Gaussian filtering procedure. A single way to characterize the complete procedure is:

$$h^d(a,b) = \frac{\sum_{(j,k)\in\aleph} V^d(j,k)h(j,k)}{\sum_{(j,k)\in\aleph} V_d(j,k)} \quad (1)$$

If low-pass filtering is complete, the Gaussian filter's output can be used as the bilateral filter's input as mentioned previously.

$$V^{dmnh}(j,k) = exp\ exp\ (-\frac{SD(a,b,j,k)_2}{2\tau_f^2})\ exp\ exp\ (-\frac{|h(a,b)-h_d(j,k)|_2}{2\tau_{e^*}^2}) \quad (2)$$

A trilateral filter under tilting can solve the problem of high-gradient zones being ineffectively filtered by bilateral filters. The tilting aspect $E\theta$ of a trilateral filter can be obtained by implementing a bilateral filter to the image data. This is because, given $E\theta$ at the target pixel, y must reject dissimilar pixels and average highly related surrounding pixels.

$$E(z) = {}^{1}\sum_{\theta} z\sum_{M\theta} xl\ a(z,x)h(l,l)_x \quad (3)_{z\ x}$$

$$E\theta = \sum z\sum x\ a(z,x)h(l_z,l_x) \quad (4)$$

The trilateral filter's $a(z)$ and $h(x)$ functions become non-orthogonal when the kernel is tilted. Each Pixel at this plane has a value that is determined by

$$B(z,x) = l(z) + E\theta.(||z-x||) \quad (5)$$

where the intensity can be represented by $l(z)$, at a target pixel, the tilting angle is $E\theta$, and the dimensional separation between z and x is denoted by $||z-x||$. The trilateral filter may smooth down high gradient zones more effectively
when the filter is tilted. It is insufficient since only tilting in areas with significant gradient changes will result in trilateral filter failure.

Dilated Leaky Shuffle Net:

Dilated Leaky ShuffleNet is a mobile-based DL architecture that is highly effective. In order to achieve more accuracy at lower computational costs, it utilized the pre-trained ShuffleNet model known as shufflenetv1 that was built using our hardware resources. The architecture consists of 172 layers in total: a softmax layer, 49 BN layers, a classification layer, 4 average pooling levels, 33 ReLU layers, and one layer for maximum pooling. To reduce the total computing complexity, the system makes use of four pooling layers.

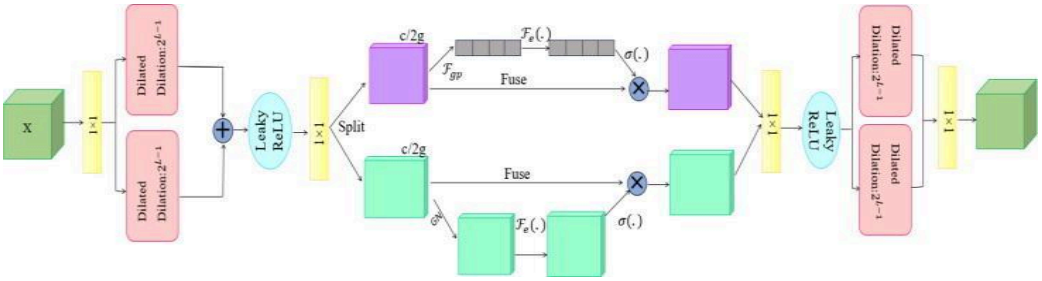

Figure 2:Architecture of Dilated Leaky Shuffle Net

The input layer, which serves as the main layer of our model processes 224 × 224 input images such as a chest radiograph. The characteristics map that convolutional layers generate is computed as

$$p(a,b) = (L\times R)(a,b) = \sum_{m}\sum_{n} A(n,m)R(a-n,b-m) \quad (6)$$

The input imagine is denoted by the letter L, the output feature map by p and the convolutional layer's kernel by R. The output with size $O = ((a-r)+2k)/(p+1)$ is obtained when the input image is subjected to convolution

processes. In this section a denotes input, k denotes padding, r denotes kernel size, and p denotes steps. In the first pointwise group convolution, the ReLU activation function, BN, and channel shuffle operation take place. Due of its simplicity and effectiveness, The Leaky ReLU has been switched on. Relu functions in the manner described follows:

$$f(y) = \{0, y < 0\ y, y \leq 0 \qquad (7)$$

Leaky ReLU employs values that are positive to turn on neural networks to turn off (set to 0) neurons. BN performs the following two and three convolution operations 2 × 3 depthwise convolution and the pointwise group convolution of size 1 x 1. The ShuffleNet units in the model are sixteen in a row. The model consists of fifty layers that provide trainable feature maps. Furthermore, characteristics are extracted by these layers. The final classification layer receives these feature maps from FC and utilizes Soft-max registration to calculate the classification probability. The FC layer's operation is represented by equation (8).

$$i_a = \sum_{b=0}^{n \times m-1} \quad v_{a,b} \times y_a + j_a \qquad (8)$$

where the values for m, n *and* g and j represent the output of the FC layer, respectively, and j stands for the output index. Additionally, the variables b and w denote the weights and bias. It focused on two, three, four, and five classes in our research, despite the fact that classification probability of the Soft-max layer can produce up to 1000 distinct classes. Functions r and f specified on the integer set X produce the i-dilated convolution provided by

$$(r *_i f)(h) = \sum_{h=-\infty}^{\infty} r(n)d(h - tm) \qquad (9)$$

The operator $*_i$ stands for the i-dilated convolution operator. CNNs and RNNs meet at the middle with the dilated convolution. This convolution uses short-distance gradient propagation to increase receptive fields exponentially without sacrificing resolution or coverage. This makes them highly suitable for applications that prioritize the cost-effective integration of knowledge about a broader context. Although the kernel window in conventional convolutions consists of neighboring input, in dilated convolutions the distance (convolution with holes) between values in the kernel window is specified. The kernel window of size r, starting at position j, and the dilation g is described as follows:

$$[y_j\ y_{j+g}\ y_{j+2g}\ y_{j+(r-1)g}] \qquad (10)$$

Dilated convolutions have enormous receptive fields with few back-propagation steps because convolutional layer stacking with increasingly dilated values allows for an exponential rise in the receptive field.

Classification:

SVM: Support vector machines (SVMs) are used to resolve classification and regression issues; they are referred to as support vector classifiers (SVC) and support vector regressions (SVR) in these two distinct contexts. SVMs can be classified into two categories: linear and non-linear SVM based on whether higher dimensions are required for the data. There are two subgroups of linear SVMs: separable and non-separable situations. For the purpose of classifying all training data points with no previous misclassification errors can construct a linear separable hyperplane. In contrast, the latter case results in the existence of a linear separable hyperplane at the cost of certain training errors.

The linearly separable and non-separable data are connected by a kernel feature. Some of the most crucial components of the kernel are.

Linear Kernel: $K(z_a, z_b) = (z_a^R z_b)$,

RBF Kernal: $K(z_a, z_b) = exp\ [|z_a - z_b||^2]$, where δ is referred to as the sigma/gamma parameter,

Sigmoid Kernel: $K(z_a, z_b) = tanh\ [(z_a^R z_b) + p]$, where p is the parameter and

Polynomial kernel: $K(z_a, z_b) = [\delta(z_a^R z_b) + 1]^d$,where h and δ are the degree and scale parameters, respectively.

The parameter δ in the reach of a training point is determined in polynomial and RBF kernels. When δ is high, the training points nearest to the boundary will be used to calculate the SVM decision boundary, while the training points farther away will be ignored.

KNN: One popular categorization method for organizing provided the KNN data divide into predefined classes (k). The straightforward process of the KNN algorithm is figuring out the Euclidean distance function between each variable sample and the pre-established classes. Based on the closest k neighbors, the samples are categorized. There

are several variations in the distance function between the samples. The Euclidean distance, which is represented by Eq. () is the most often utilized.

$$g = \sqrt{\sum_{f=1}^{m} (Y_{1f} - Y_{2f})^2} \quad (11)$$

where Y_1,Y_2 are the input samples and f is the number of values in each sample vector. When the number of neighbors drops, the classifier's accuracy increases.

Random Forest: The RF technique was developed by to address regression and classification issues is an ensemble learning technique. Using several models to address a single problem, ensemble learning is a machine learning technique that increases accuracy. Specifically, ensemble classification uses several classifiers to get findings that are more accurate than those of a single classifier. In simpler terms, combining several classifiers reduces variation and can lead to more dependable outcomes, particularly when dealing with unstable classifiers. After this, a voting scenario is created to give unlabelled samples a label. A popular voting strategy is majority voting, which gives each unlabelled sample the label that receives the greatest number of votes from different classifiers. The majority voting method's simplicity and efficacy are the reasons behind its popularity.

Decision Tree: Many algorithms for building decision trees have been proposed. This experiment uses a supervised learning method called Decision Tree Classifier. It may be used to create both regression and classification trees, and it is based on CART. The majority of the concepts in the CART model are implemented by the R programming package rpart. GINI index and information gain were applied to create several classification models.

RESULT AND DISCUSSION:

This section analyzes performance in terms of several evaluation criteria and looks at the assessment outcomes of the osteoporosis detection. This osteoporosis detection and classification is found using the Python programming language and libraries (Sci-Kit-Learn, TensorFlow, Keras, Numpy, HDF5, etc.) on an Intel Core i7 processor running Windows with 16 GB of RAM.

Dataset Description

OsteoLaus Dataset [27]: OsteoLaus Dataset is a comprehensive and meticulously curated dataset derived from research on osteoporosis and bone health conducted in the Lausanne cohort. This dataset comprises imaging, clinical, and demographic information for the research of bone mineral density (BMD) and associated disorders. It is a subset of the OsteoLaus cohort that focuses on how menopause affects bone health, especially when it comes to osteoporosis.

Performance Analysis:

Evaluation measures were employed to verify the efficacy and characteristics of the proposed approach. True Positive ($True^+$), True Negative ($True^-$), False Positive ($False^+$), and False Negative ($False^-$) are the four basic metrics that are commonly used to assess performance. Accuracy refers to the detecting system's ability to osteoporosis detection. The following expression was used to calculate the accuracy.

$$Accuracy = \frac{True^+ + True^-}{True^+ + True^- + False^+ + Fals_{e^-}} \quad (12)$$

Precision, which describes the accurate way a model can categorize a positive outcome, is another name for positive predictive ability

$$Precision = \frac{True+}{True+ + False+} \quad (13)$$

The recall measure indicates how well the system finds outcomes. Another other word for sensitivity is recall

$$Recall = \frac{True+}{True+ + False-} \quad (14)$$

The harmonic means of recall and precision, or F1-Score, can be obtained using the following formula:

$$F1\ Score = \frac{2}{(\quad)+(\quad)} \quad (15)$$

Whereas $False^{+}$ and $False^{-}$ indicate false positives and negatives. $True^{+}$ and $True^{-}$ indicate real positives and negatives. The following table demonstrates the proposed method for detecting and classifying the osteoporosis.

Classes	Accuracy	Precision	Recall	F1-Score
Normal	99.76 %	97.43 %	98.18%	97.98 %
Abnormal	99.89%	96.81 %	98.42%	96.85%

Table 1 presents an evaluation criteria of the proposed approach for classifying the osteoporosis classes. The proposed OSIS-NET method is evaluated using accuracy, precision, recall, and F1-Score, each of which has an overall value of 99.83%, 97.12%, 98.30%, and 97.42% respectively.

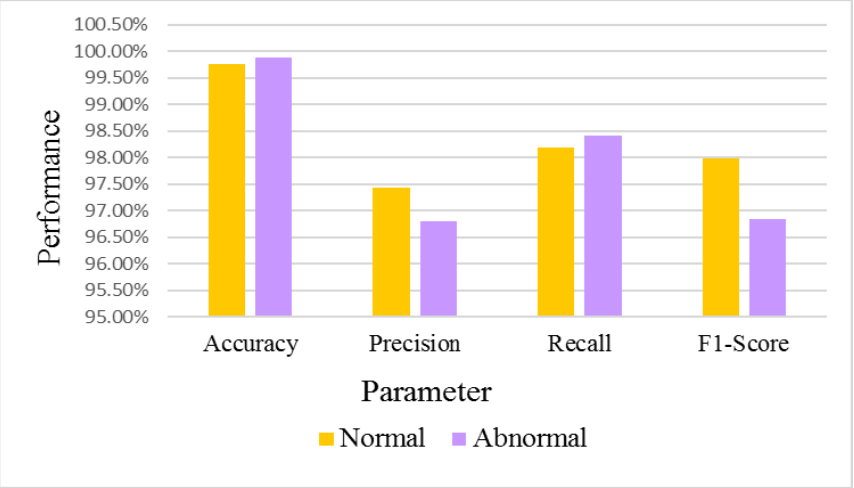

Figure 3: Performance of the Proposed Method.

Figure 3 displays the performance of the proposed OSIS-NET method. The proposed method achieves an accuracy rate of 99.76% in the normal and 99.89% in the abnormal classes. It attain an overall accuracy rate of 99.83%.

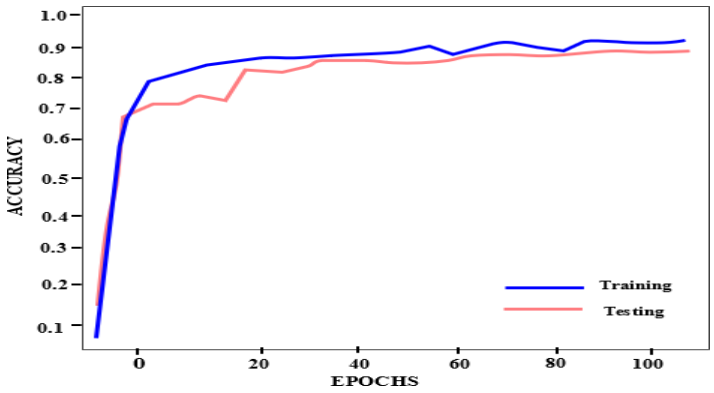

Figure 4: Accuracy graph of the proposed OSIS-NET method.

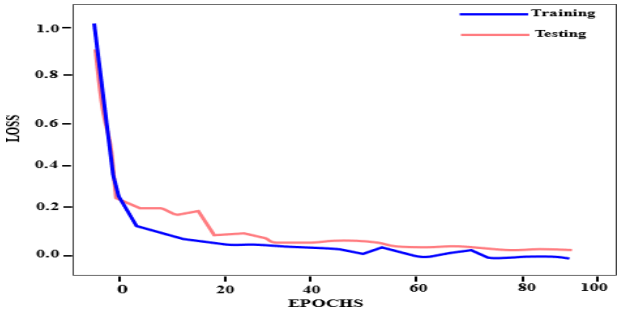

Figure 5: Loss graph of the Proposed OSIS-NET method.

Figure 4 illustrate the excellent accuracy attained by the proposed model in both training and testing while figure 5 illustrate the loss. The accuracy of the proposed OSIS-NET Method is 99.83%.

Comparative Analysis:

This section illustrates that the proposed OSIS-NET approach compares effectively to the current neural networks. The effectiveness of the proposed approach was evaluated using accuracy, precision, recall and F1-Score measures.

Table 2: Comparison with other Neural Network.

Network	Accuracy	Precision	Recall	F1-Score
GoogleNet [23]	98.97%	95.84%	96.46%	96.26%
ShuffleNet [24]	99.29%	94.64%	97.15%	95.84%
AlexNet [25]	99.67%	96.88%	96.54%	96.62%
MobileNet [26]	98.76%	95.28%	95.78%	94.90%
Dilated Leaky Shuffle Net (Proposed)	99.83%	97.12%	98.30%	97.42%

Table 2 shows the comparison of another traditional deep neural network with the proposed Dilated Leaky Shuffle Net. The proposed Dilated Leaky Shuffle Net outperform highest accuracy rate than another traditional network. It improves the overall accuracy by 0.86%, 0.54%, 0.16% and 1.07% better than the GoogleNet, ShuffleNet, AlexNet and MobileNet respectively.

Ablation Study:

An ablation study was made to asses the efficiency of the Dilated leaky Shuffle Net and Standard Shuffle Net utilized in selecting the most relevant features. The classification accuracy for Normal and Abnormal osteoporosis detection and classification in this experiment is shown in Table 3.

Table 3: Ablation Study for Standard Leaky shuffle Net and Dilated Leaky Shuffle Net.

Classes	Without Standard Leaky Shuffle Net	With Standard Leaky Shuffle Net	Without Dilated Leaky Shuffle Net	With Dilated Leaky Shuffle Net
Accuracy	98.46%	99.15%	99.31%	99.83%
Precision	95. 85%	96.84%	97.03%	97.12%
Recall	97.28%	97.64%	97.94%	98.30%
F1-Score	96.13%	96.87%	96.86%	97.42%

Standard Leaky shuffle Net and Dilated Leaky shuffle Net are well-known technology in feature extraction process. In this ablation study the Dilated Leaky Shuffle Net attains highest accuracy, Precision and Recall and F1 -Score values.

Table 4: Comparison of proposed with Existing Method

Author	Technique	Accuracy
Liu, J., et al [16]	U-Net	98.65%
Fang, Y., et al [17]	DCNN	97.97%
Hwang, D.H., et al [22]	MVCTNet	98.52%
Proposed	OSIS-NET	99.83%

According to table 4 : the proposed OSIS-NET improves the overall truth by 1.18%, 1.86% and 1.31% better than U-NET, DCNN and MVCTNet respectively. Based on the above comparison the proposed OSIS-NET model is more accurate than the existing methods.

CONCLUSION

This research proposes OSIS-NET as a tool to identify and sort osteoporosis cases through deep learning procedures. We obtain MRI scans from OASIS-3 Data and apply adaptive gaussian trilateral filter before processing to remove noise. The input images go through the Sobel edge detector for creating precise and fine edge details in both images. DL-based Dilated leaky ShuffleNet receives the input images to capture both textural and shape features from these inputs. The picked ST attributes undergo evaluation through different machine learning solutions including SVM, KNN, DT and RF to distinguish healthy from damaged situations. The system generates 99.76% correct results for normal images and 99.89% accuracy for medical image defects. Because of its design the method boosts accuracy levels more extensively than GoogleNet (0.86%), ShuffleNet (0.54%), AlexNet (0.16%) and MobileNet (1.07%).

REFERENCES:

[1] Liu, P., Liang, X., Li, Z., Zhu, X., Zhang, Z. and Cai, L., 2019. Decoupled effects of bone mass, microarchitecture and tissue property on the mechanical deterioration of osteoporotic bones. Composites Part B: Engineering, 177, p.107436.

[2] Li, Z., Liu, P., Yuan, Y., Liang, X., Lei, J., Zhu, X., Zhang, Z. and Cai, L., 2021. Loss of longitudinal superiority marks the microarchitecture deterioration of osteoporotic cancellous bones. Biomechanics and Modeling in Mechanobiology, 20, pp.2013-2030.

[3] Demir, B., Haberal, A., Geyik, P.I.N.A.R., Baskan, B., Ozturkoglu, E., Karacay, O. and Deveci, S., 2008. Identification of the risk factors for osteoporosis among postmenopausal women. Maturitas, 60(3-4), pp.253-256.

[4] Hernandez, C.J., Beaupre, G.S. and Carter, D.R., 2003. A theoretical analysis of the relative influences of peak BMD, age-related bone loss and menopause on the development of osteoporosis. Osteoporosis international, 14, pp.843-847.

[5] Rao, D.T., Ramesh, K.S., Ghali, V.S. and Rao, M.V., 2022. The osteoporosis disease diagnosis and classification using U-Net deep learning process. Journal of Mobile Multimedia, pp.1131-1152.

[6] Yamamoto, N., Sukegawa, S., Kitamura, A., Goto, R., Noda, T., Nakano, K., Takabatake, K., Kawai, H., Nagatsuka, H., Kawasaki, K. and Furuki, Y., 2020. Deep learning for osteoporosis classification using hip radiographs and patient clinical covariates. Biomolecules, 10(11), p.1534.

[7] Nakamoto, T., Taguchi, A. and Kakimoto, N., 2022. Osteoporosis screening support system from panoramic radiographs using deep learning by convolutional neural network. Dentomaxillofacial Radiology, 51(6), p.20220135.

[8] Peng, T., Zeng, X., Li, Y., Li, M., Pu, B., Zhi, B., Wang, Y. and Qu, H., 2024. A study on whether deep learning models based on CT images for bone density classification and prediction can be used for opportunistic osteoporosis screening. Osteoporosis International, 35(1), pp.117-128.
[9] Patil, K.A., Prashanth, K.M. and Ramalingaiah, A., 2021. A comparative study on detection of osteoporosis using deep learning methods: A review. International Journal of Orthopaedics Sciences, 7(3), pp.108-115.
[10] Wong, C.P., Gani, L.U. and Chong, L.R., 2020. Dual-energy X-ray absorptiometry bone densitometry and pitfalls in the assessment of osteoporosis: a primer for the practicing clinician. Archives of Osteoporosis, 15, pp.1-11.
[11] Eirini, K., Nikolaos, T., Papadopoulou, S.K. and Georgios, G., 2022. Bone Density Measurements and Biomarkers in Nutrition: DXA (Dual X-ray Absorptiometry), Osteopenia, and Osteoporosis. In Biomarkers in Nutrition (pp. 1067-1084). Cham: Springer International Publishing.
[12] Viswanathan, M., Reddy, S., Berkman, N., Cullen, K., Middleton, J.C., Nicholson, W.K. and Kahwati, L.C., 2018. Screening to prevent osteoporotic fractures: updated evidence report and systematic review for the US Preventive Services Task Force. Jama, 319(24), pp.2532-2551.
[13] Pfister, A.K., Welch, C.W. and Emmett, M., 2011. Screening for osteoporosis: US preventive services task force recommendation statement. Annals of internal medicine, 155(4), pp.275-276.
[14] Bansal, S., Pecina, J.L., Merry, S.P., Kennel, K.A., Maxson, J., Quigg, S. and Thacher, T.D., 2015. US Preventative Services Task Force FRAX threshold has a low sensitivity to detect osteoporosis in women ages 50–64 years. Osteoporosis International, 26, pp.1429-1433.
[15] Ulivieri, F.M. and Rinaudo, L., 2021. Beyond bone mineral density: a new dual X-ray absorptiometry index of bone strength to predict fragility fractures, the bone strain index. Frontiers in Medicine, 7, p.590139.
[16] Aliaga, I., Vera, V., Vera, M., García, E., Pedrera, M. and Pajares, G., 2020. Automatic computation of mandibular indices in dental panoramic radiographs for early osteoporosis detection. Artificial intelligence in medicine, 103, p.101816.
[17] Liu, J., Wang, J., Ruan, W., Lin, C. and Chen, D., 2020. Diagnostic and gradation model of osteoporosis based on improved deep U-Net network. Journal of medical systems, 44(1), p.15.
[18] M. Yogeshwari, G.Thailambal, “Automatic Fearture extraction and detection of plant leaf disease using GLCM features and Convolutional Neural Network”, Elsevier, Science Direct 2021.
[19] M. Yogeshwari, G.Thailambal, “Automatic segmentation of plant leaf disease using improved fast fuzzy C means clustering and adaptive otsu thresholding(IFFCM-AO) algorithm”, European Journal of Molecular & Clinical Medicine(EJMCM),Volume 7, 2020.
[20] Pulla Sujarani, M. Yogeshwari, “Comparative Study of Cancer Blood Disorder Detection Using Convolutional Neural Networks” published in "Recent Developments in Machine and Human Intelligence" IGIG, DOI: 10.4018/978-1-6684-9189-8.ch009. (Scopus Indexed)
[21] Pulla Sujarani, M. Yogeshwari “A Novel Image Filtering and Enhancement Techniques for the Detection of Cancer Blood Disorder” Submitted to Advances in Science, Technology & Innovation, Springer, ASCIS 2023, pp. 140–153, no2024. DOI:10.1007/978-3-031-59097-9_11. (Scopus Indexed)
[22] Pulla Sujarani, M. Yogeshwari, k. kalaiselvi, “Early Identification of Cancer Blood Disorder using Deep Convolutional Neural Networks” Published in ACM Journal, ICIMMI ‘23, pp-1-4, November 2023, DOI: 10.1145/3647444.3647956. (Scopus Indexed)
[23] Pulla Sujarani, M. Yogeshwari, “Utilising Deep Convolutional Neural Networks and Hybrid Clustering Techniques for Predicting Cancer Blood Disorder”, Published in International Journal of Bioinformatics Research and Applications (IJBRA), Vol.19, No.5-6, pp- 462-486, 2023, DOI:10.1504/IJBRA.2023.139121. (Scopus Indexed)
[24] Pulla Sujarani, k. kalaiselvi, M. Yogeshwari “Prediction of Blood Disorder and Cancer using Artificial Neural Networks: A Review”, published in Journal of Chemical Health Risks (JCHR), 14(2), pp.357-363, ISSN: 2251-6727, 2024.
[25] D.Padma Priya, Sathya P.bS., Nisha M.C, Vasumathi B.D, Priya, Vishwa V.E, and Yogeshwari.M (2025). AI-Driven Predictive Analytics for Early Disease Detection Leveraging Body Sensor Networks and Advanced Machine Learning Models. Journal of Information Systems Engineering and Management, 10, 279 - 292. https://doi.org/10.52783/jisem.v10i12s.1810
[26] Devi, S. Rukmani (58489473100); Raghi, K.R. (59000167600); Priya, S. Geetha (59268127200); Sathi, G. (57723269500); Kumar, Sarva Naveen (58510197200); Dinesh, M. (58924627800)Design and Development of a Touch Free Smart Home Controlling System Based on Virtual Reality (VR) Technology202410.1109/ISCS61804.2024.10581017
[27] Senthil Kumar, K. (57212285315); Rukmani Devi, S. (58489473100); Ranjan, Nidhi (58614379800); Rath, Gitika (59009846100); Indira, G. (36902715100); Nishant, Neerav (58296471900)Deploying Hybrid MAELM Approach for Human Emotion Detection Through Speech and Facial Expressions202310.1109/ICIMIA60377.2023.10426605